42nd AIAA/ASME/SAE/ASEE Joint Propulsion Conference & Exhibit
9 - 12 July 2006, Sacramento, California

AIAA 2006-5026

Particle Simulation of Plume Flows From an Anode Layer Hall Thruster

Yongjun Choi*, Michael Keidar† and Iain D. Boyd‡
University of Michigan, Ann Arbor, MI 48109

In this study, 2D simulations of xenon plasma plume flow fields from a D55 anode layer Hall thruster are performed with a hybrid particle-fluid method. In this simulation, the Boltzmann model and a detailed fluid model are used to compute the electron properties, the direct simulation Monte Carlo method models the collisions of heavy particles, and the Particle In Cell method models the transport of ions in electric fields. The accuracy of the simulation is assessed through comparison with available measured data. The simulation employing the detailed electron fluid model successfully captures detailed plume structures both in the near and far fields.

Nomenclature

c_e	=	mean electron thermal velocity
C_i	=	ionization coefficient
e	=	unit charge
$\vec{E}$	=	electric field
g	=	relative velocity
$\vec{j}$	=	current density
k	=	Boltzmann constant
m_c	=	reduced mass
m_e	=	electron mass
m_i	=	ion mass
n	=	plasma number density
n_n	=	neutral number density
n_{ref}	=	reference plasma number density
P_e	=	electron pressure
T_e	=	electron temperature
T_H	=	heavy particle temperature
$\overrightarrow{V_e}$	=	electron velocity vector
σ	=	plasma conductivity
σ_i	=	reference cross section for xenon
κ_e	=	electron thermal conductivity
ε_i	=	ionization energy
ϕ	=	plasma potential
ϕ_{ref}	=	reference plasma potential
ν_e	=	electron collision frequency
ν_{ei}	=	ion-electron collision frequency
ν_{en}	=	neutral electron collision frequency
Ψ	=	electron stream function

* Graduate student, Department of Aerospace Engineering, AIAA Student Member.

† Assistant Research Scientist, Department of Aerospace Engineering, AIAA Senior Member.

‡ Professor, Department of Aerospace Engineering, AIAA Associate Fellow.

I. Introduction

Hall effect thrusters represent an efficient form of electric propulsion devices for applications requiring low thrust levels, e.g. station-keeping, orbit raising, and orbit transfers. In a Hall thruster, ions are accelerated by electric fields and used to generate propulsive thrust. The energy required to accelerate ions is obtained from on-board batteries or solar cells. Hall thrusters are able to perform better than chemical propulsion systems because Hall thrusters can obtain electricity input directly in space through solar cells, do not need to carry any oxidizer, and so allow a larger payload. Furthermore, Hall thrusters can realize much higher propellant exhaust velocities than chemical propulsion systems, thereby achieving higher impulse from a given propellant mass and making the use of Hall thrusters for interplanetary missions feasible.

In the past years, two types of Hall thrusters were developed: a thruster with closed electron drift and extended acceleration zone, or Stationary Plasma Thruster (SPT), and a thruster with a very short acceleration channel, or Thruster with Anode Layer (TAL). The SPT employs a relatively long acceleration channel and ceramic wall insulator materials, such as boron nitride or silicon carbide. The TAL employs a shorter acceleration channel and conducting metallic wall materials which are typically stainless steel or molybdenum.

Among Hall thruster technologies, TAL, which was developed in the 1960's at TsNIIMASH, seems to be advantageous for two reasons. First, TAL has a very short acceleration zone (a few millimeters) and so there is less contact of ions with thruster surfaces; hence, it is favorable for long-term missions because of a reduction in erosion of thruster components. Second, higher power Hall thrusters will be needed in future space missions and a TAL with very high power has been specially developed to meet this requirement.[1]

The plume, especially the near field plume, of a Hall thruster is a physically complex region and very important because data obtained in the near-field provide information of the thruster's internal flow and its far field plume where it is much more difficult to obtain data directly from these two areas. So, accurate simulation of the plume fields emitted from Hall thrusters is needed. Furthermore, the plume fields yield information helpful on understanding the plume impingement that involves fluxes of high-energy ions and charge-exchanged particles onto sensitive spacecraft devices such as solar cells. Therefore, understanding the behavior of the thruster plume is very important to design thrusters and spacecraft.

A plasma plume is a complex rarefied flow with several species: atoms, positively charged ions, and electrons. Generally, a hybrid particle-fluid approach is used for the computational simulation of plasma plume flow into vacuum. The direct simulation Monte Carlo (DSMC) method[2] simulates the collisions of heavy particles (ions and atoms), and the Particle-In-Cell (PIC) technique[3] models the transport of ions in electric fields. Electrons are treated using a fluid description, because electrons, which have significantly lighter mass, can adjust their velocities more quickly than ions or atoms**.**

For the electron fluid model, usually the *Boltzmann* relation is adopted.[4, 5] The *Boltzmann model* provides the plasma potential using several strong assumptions such as a constant electron temperature for a whole domain. The *Detailed model* which has been developed recently,[6] is based on the conservation laws for electrons and is capable of representing accurate and detailed distributions for electron temperature, plasma potential and electron velocity. This model was successfully applied in a simulation of an axi-symmetric plasma plume from a 200W class SPT-type Hall thruster[6] and in another simulation of 3D plasma plumes from a cluster of four 200 W class Hall thrusters.[7]

In this study, the 2D axi-symmetric plume flow fields from a D55 TAL Hall thruster are investigated using MONACO,[8] a hybrid PIC-DSMC code developed at the University of Michigan with both the *Boltzmann model* and the *Detailed model*.

Section II reviews numerical models, and brief information for experiments and flow conditions. Section III presents general features of the numerical 2D simulation results and a comparison of these results with experimental data taken in the plume of the D55.

II. Models and Flow Conditions

A. Plasma Dynamics

For particle simulation of plume flows, heavy neutrals and ions are modeled with the DSMC-PIC method, and the electrons are assumed as a fluid because electrons adjust their velocities more quickly with their significantly lighter mass.

The simplest fluid electron model is the *Boltzmann* relation

$$\phi = \phi_{ref} + \frac{kT_{ref}}{e} \ln\left(\frac{n_e}{n_{ref}}\right) \tag{1}$$

This equation is derived using several assumptions including that the electron flow is isothermal, collisionless, obeys the ideal gas law, and the magnetic field is neglected.

Recently, a *Detailed model* was proposed[6] which represents a significantly increased level of physics compared to the *Boltzmann model*. In the *Detailed model*, the electron continuity equation is transformed into a Poisson equation by assuming steady flow and introducing a stream function;

$$\nabla^2 \Psi = C_i n_e n_i \tag{2}$$

The xenon ionization rate coefficient is expressed as a function of electron temperature using a relation proposed by Ahedo[9]

$$C_i = \sigma_i c_e \left(1 + \frac{T_e \varepsilon_i}{(T_e + \varepsilon_i)^2}\right) \exp\left(-\frac{\varepsilon_i}{T_e}\right) \tag{3}$$

From the generalized Ohm's law, we can obtain an equation for the plasma potential

$$\nabla\bullet(\sigma\nabla\phi) = \frac{k\sigma}{e}\left(\nabla^2 T_e + T_e \nabla^2(\ln n_e)\right) + \sigma\nabla(\ln n_e)\bullet\nabla T_e + T_e \nabla\sigma\bullet\nabla(\ln n_e + \nabla\sigma\bullet\nabla T_e) \tag{4}$$

The electron temperature equation is obtained from the steady state electron energy equation

$$\nabla^2 T_e = -\nabla \ln \kappa_e \bullet \nabla T_e + \frac{1}{\kappa_e}\left(-\vec{j}\bullet\vec{E} + \frac{3}{2} n_e (\vec{V}_e \bullet \nabla) k T_e + p_e \nabla\bullet\vec{V}_e + 3\frac{m_e}{m_i} \nu_e n_e k (T_e - T_H) + n_e n_i C_i \varepsilon\right) \tag{5}$$

The electron number density n_e is set equal to the ion number density n_i based on the plasma quasi-neutral assumption. The electron conductivity σ, the electron thermal conductivity κ_e, the ion-electron collision frequency ν_{ei}, and the neutral electron collision frequency ν_{en} can be found in ref. 10.

$$\sigma = \frac{e^2 n_e}{m_e \nu_e} \tag{6}$$

$$\kappa_e = \frac{2.4}{1 + \frac{\nu_{ei}}{\sqrt{2}\nu_e}} \frac{k^2 n_e T_e}{m_e \nu_e} \tag{7}$$

By treating the right hand side terms as known sources and solving Eqs. (2, 4, 5), three fundamental electron properties are obtained, i.e., electron velocity, plasma potential, and electron temperature. With these detailed properties, the plasma plume simulation yields much improved results in comparison to the *Boltzmann model* for the plume of an SPT-type Hall thruster.[6]

B. Collision Dynamics

Two types of collisions are important in the Hall thruster: elastic (momentum exchange) and charge exchange (CEX). There are two kinds of elastic collisions: atom-atom and atom-ion interactions. For atom-atom collisions, the Variable Hard Sphere[2] model is used and the collision cross section for xenon is

$$\sigma_{el}\left(\mathbf{Xe,Xe}\right)=\frac{2.12\times10^{-18}}{g^{2\omega}} \tag{8}$$

where g is the relative velocity and ω=0.12 is related to the viscosity temperature exponent for xenon. For atom-ion elastic collisions, the MEX cross section is set equal to the CEX cross section.

Charge exchange concerns the transfer of one or more electrons between an atom and an ion. For single charged ions, we use the following cross section measured by Pullins et al.[11] and Miller et al.[12]

$$\sigma_{cex}\left(\mathbf{Xe,Xe^{+}}\right)=1.1872\times10^{-20}\left(142.21-23.30\log\left(g\right)\right) \tag{9}$$

Also, Refs. 11 and 12 reported that the CEX cross section for double charged ions is approximately half as large as single charged ions at corresponding energies.

C. Flow Conditions

The device considered in the present study is the D55 TAL Hall thruster developed by TsNIIMASH. We have chosen to study the D55 Hall thruster because of the availability of a significant amount of experimental data for this device. A schematic of the D55 thruster is presented in Fig. 1.

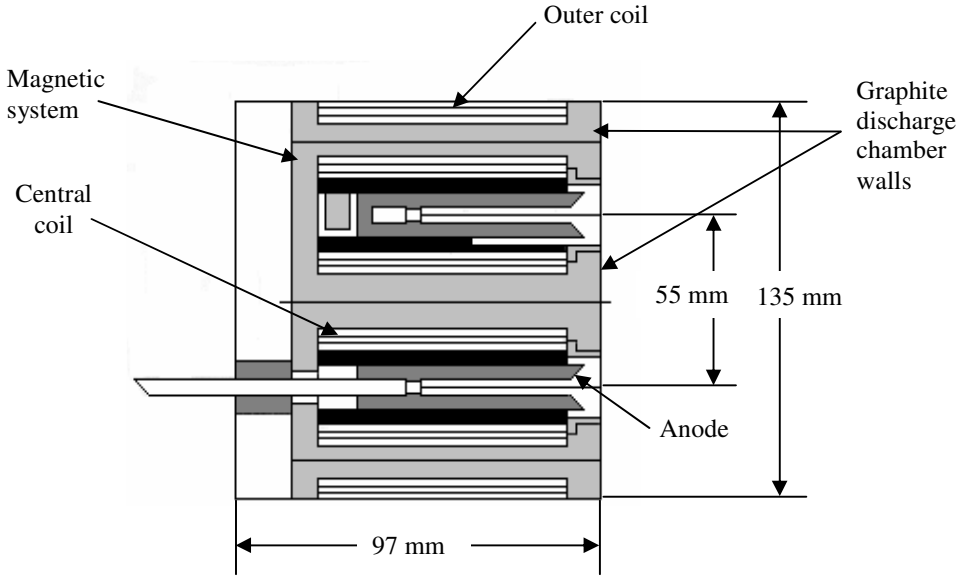

Figure 1. Schematic of the D55 anode-layer Hall thruster.

We consider three conditions corresponding to three different experiments. Most of the results presented here are for a series of experiments conducted at the University of Michigan.[13, 14] The D55 thruster was operated at a flow rate of 4.76 mg/s of xenon, a discharge voltage of 300 V, and a current of 4.5 A. The specific impulse under these conditions was previously measured to be 1,810 s.[15] For the D55 thruster, it is known that a portion of the thrust is generated outside the thruster, so we adopt 145 V of plasma potential. With this plasma potential, the thrust from the thruster itself is 80 % of the total thrust. The fraction of double xenon ions is assumed to be 0.25. At the thruster exit, the electron temperature is taken to be 10 eV in the *Boltzmann model* and the *Detailed model*, the temperature of the ions is assumed to be 4 eV, and that of the neutrals is assumed to be 750 K. The D55 has a nozzle-like geometry at the exit, so the plume spreads at the thruster exit with certain angles. In the present study, we adopt 15 deg as a half angle, and the radial velocity varies linearly across each half of the exit plane. The backpressure in the Michigan facility is reported as 8.3 x 10^{-3} Pa.

The second flow condition investigated corresponds to a study performed by TsNIIMASH.[16] The thruster was operated at a flow rate of 3.5 mg/s and a current of 3 A. The background pressure with the thruster running was 5.9 x 10^{-3} Pa.

The third flow condition corresponds to a study performed by the University of Tennessee Space Institute (UTSI) and Lockheed Martin Astronautics (LMA).[17] The thruster was operated at a flow rate of 6 mg/s and a current of 4.5 A. The background pressure with the thruster running was 9.3 x 10^{-3} Pa.

The computational domain extends to 1.1 m downstream from the thruster exit plane, to 0.67 m radially, and a small portion of the back flow region is also included. The computational grid employed in the present study consists of rectangular cells. The smallest cells are located close to the thruster exit and have a size of 5 mm. The largest cells are those close to the edges of the domain and have a size of 1 cm. The computations presented in the study typically employed 500,000 particles with a total of 60,000 time steps. Table 1 is a listing of the flow conditions assumed at the thruster exit.

Experiment	species	n, m^{-3}	T, K	U, m/s
Michigan	Xe	$3.8x10^{18}$	750	281
	Xe^{+}	$3.6x10^{17}$	46,400	15,000
	Xe^{++}	$9.0x10^{16}$	46,400	21,300
TsNIIMASH	Xe	$4.6x10^{18}$	750	281
	Xe^{+}	$2.4x10^{17}$	46,400	15,000
	Xe^{++}	$6.0x10^{16}$	46,400	21,300
UTSI & LMA	Xe	$1.2x10^{19}$	750	281
	Xe^{+}	$3.6x10^{17}$	46,400	15,000
	Xe^{++}	$9.0x10^{16}$	46,400	21,300

Table 1. Flow properties assumed at thruster exit plane.

III. Results

Overall plasma potential fields obtained with the *Boltzmann model* and the *Detailed model* are presented in Figs. 2a and 2b, respectively. It is known that the plasma potential fields of the *Boltzmann model* and the *Detailed model* are very different.[6] We can see similar features in Figs. 2a and 2b. The *Boltzmann model* gives weaker gradients in plasma potential, and the overall variation in potential is only about 30V.

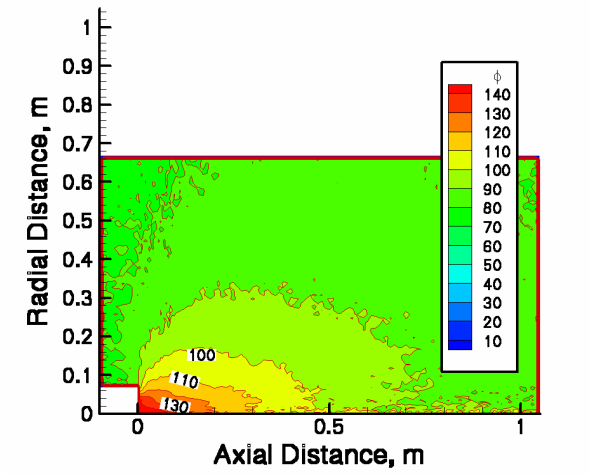

Figure 2a. Plasma potential (V) profiles computed using the Boltzmann model.

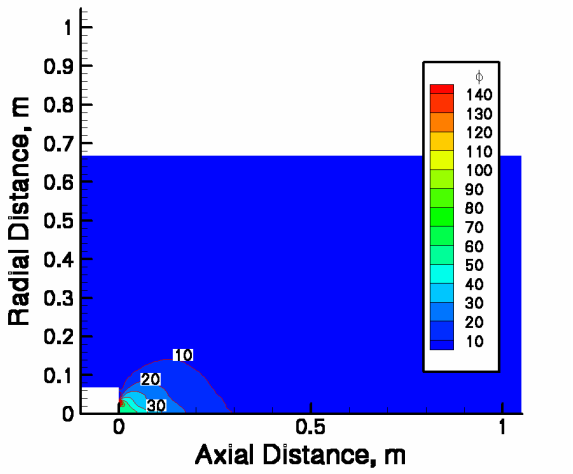

Figure 2b. Plasma potential (V) profiles computed using the detailed model.

By comparison, the potential gradients and electric fields associated with the *Detailed model* are much stronger, with a total variation in potential of about 140V. Hence, the *Detailed model* produces significantly greater ion acceleration. This feature will be discussed later.

A series of probe experiments were performed by Domonkos et al.[13] in the near field of the D55 plume. The local plasma potential was obtained using an emissive probe and a Langmuir probe; ion current density was obtained using a Faraday probe; and the electron temperature and number density were obtained using a Langmuir probe.

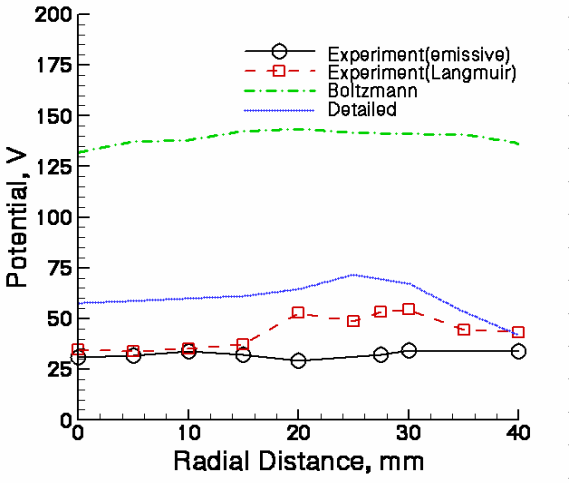

Figure 3a. Radial profiles of plasma potential at 10 mm from the thruster exit plane.

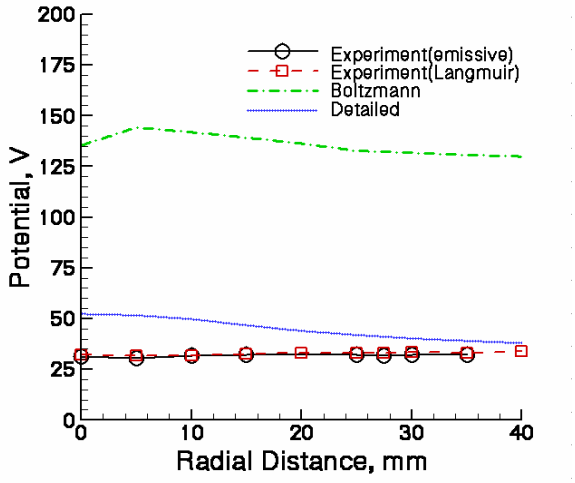

Figure 3b. Radial profiles of plasma potential at 50 mm from the thruster exit plane.

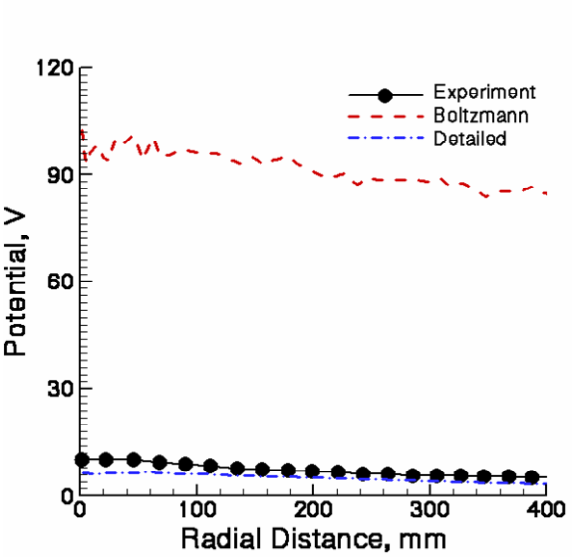

Figure 4. Radial profiles of plasma potential at 500 mm from the thruster exit plane.

Figures 3a and 3b show radial profiles of plasma potential at axial distances of 10 mm and 50 mm from the thruster exit plane, respectively. Data were measured with respect to the cathode potential of 14 V, so here we added 14V to the measured data for consistency with the simulation. Close to the thruster, the *Boltzmann model* and the *Detailed model* overpredict the potential. At 10 mm, the *Detailed model* shows the plasma potential increasing in the region of the discharge chamber and we can see that the *Detailed model* captures the shape quite well. At 50 mm from the thruster, the *Boltzmann model* still greatly overpredicts the potential, but the *Detailed model* results and measured data are in better agreement.

Comparisons between measured data and simulation results for the potential in the far-field plume are shown in Fig. 4. The measured data were obtained by Zakharenkov et al.[16] and the simulations use the second set of operating conditions given in Table 1. At a distance of 500 mm from the thruster, the *Boltzmann model* again greatly overpredicts the potential whereas the *Detailed model* reproduces fairly well the measured profiles.

Ion current density profiles predicted by the simulation are compared with the experimental data[13] in Figs. 5a and 5b along radial lines located 10 and 40 mm from the thruster exit plane, respectively. The *Boltzmann model* greatly underpredicts the measured values at 40mm but the *Detailed model* shows excellent agreement with experimental measurement.

Figure 6 shows further comparisons between measured data[16] and simulation results for ion current density in the far-field plume. The *Detailed model* shows better agreement with the measurements though both models underpredict the measured values. This underprediction of the current density in the far field implies a possibility that ionized particles are overaccelerated in the radial direction in the simulation. This feature is consistent with the comparison of far field potential and electron number density shown in Fig. 4 and Fig. 8, respectively. This feature will be discussed later.

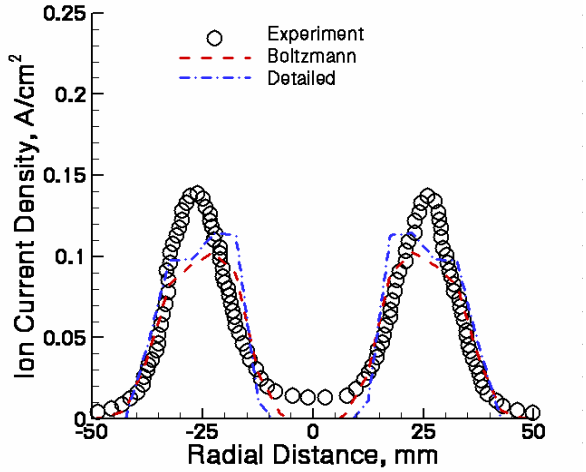

Figure 5a. Radial profiles of ion current density at 10 mm from the thruster exit plane.

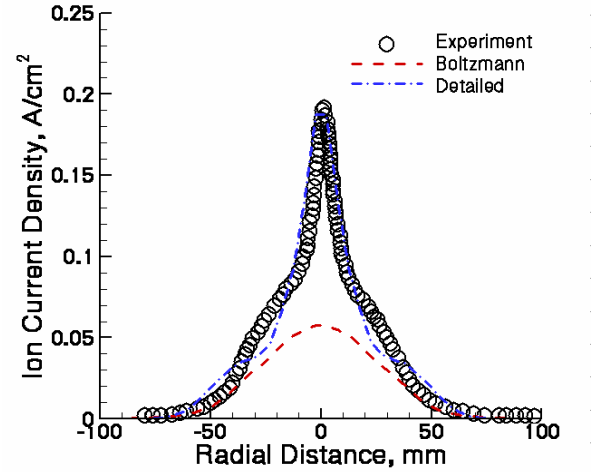

Figure 5b. Radial profiles of ion current density at 40 mm from the thruster exit plane.

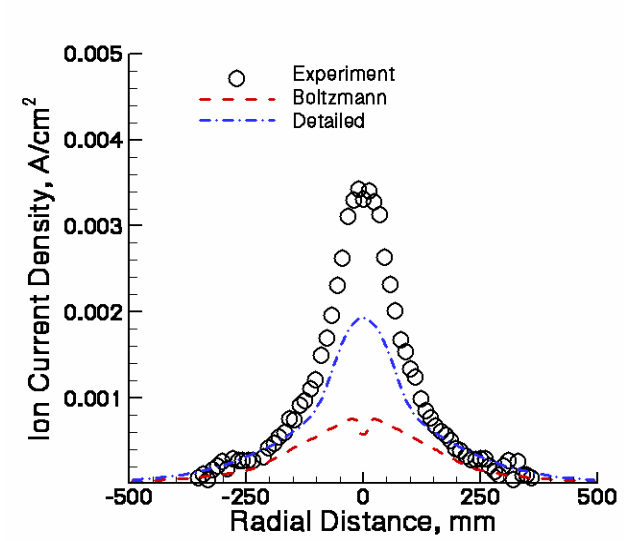

Figure 6. Radial profiles of ion current density at 500 mm from the thruster exit plane.

Measurements of electron number density[13] are compared with the simulations for radial profiles at 10 and 50 mm in Figs. 7a and 7b, respectively. The simulation values represent the total charge density obtained from the number densities of the Xe^+ and Xe^{++} ions. The measured data have an accuracy of ±50 percent at 10 and 50 mm. Therefore, in the near field, most of the simulation data are within the range although they show a tendency to underpredict the measured values.

Further comparisons between measured data and simulation results for electron number density in the far-field plume are shown in Figs 8a and 8b. The measured data were obtained by Gulczinski et al.[14] using microwave interferometry and the simulations use the first set of operating conditions given in Table 1. The uncertainty for these data is ±10 percent. The *Detailed model* shows better agreement with measurements though both models still underpredict the measured values over the entire radial profile. One possible reason for these differences between the simulation and the experiment is that the electric fields in the simulation accelerate the ions too much in both the axial and radial directions. It is known that the magnetic field leaked from the thruster is strong enough to affect the electron motion in the near-field plume region.[18] So, one way to address this difference would be to include partial confinement of electrons caused by the magnetic field of the thruster leaking into the near-field plume. This idea is consistent with the comparison of far field potential shown in Fig. 4 where the simulation predicts lower values than those measured.

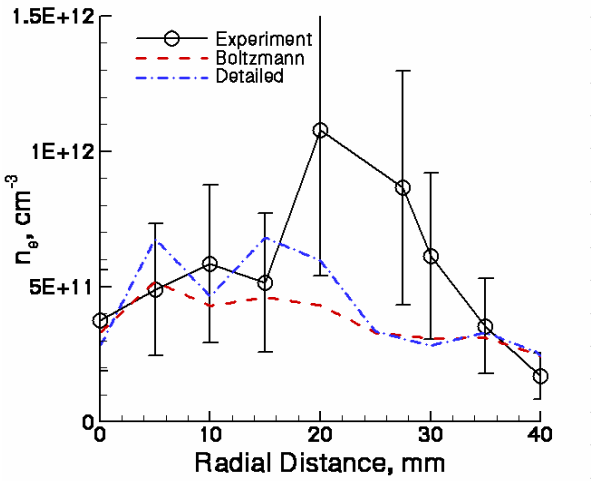

Figure 7a. Radial profiles of electron number density at 10 mm from the thruster exit plane.

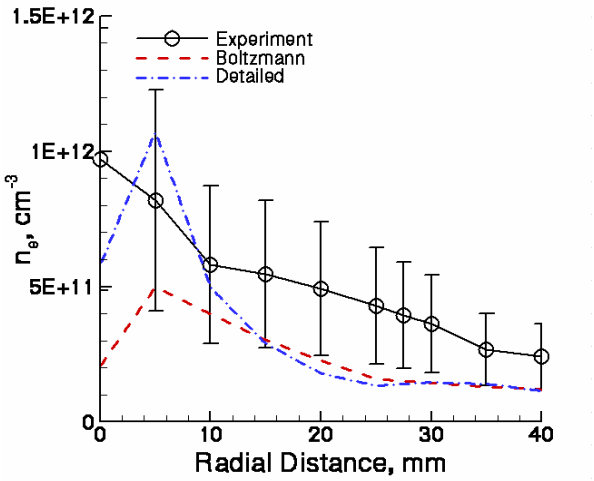

Figure 7b. Radial profiles of electron number density at 50 mm from the thruster exit plane.

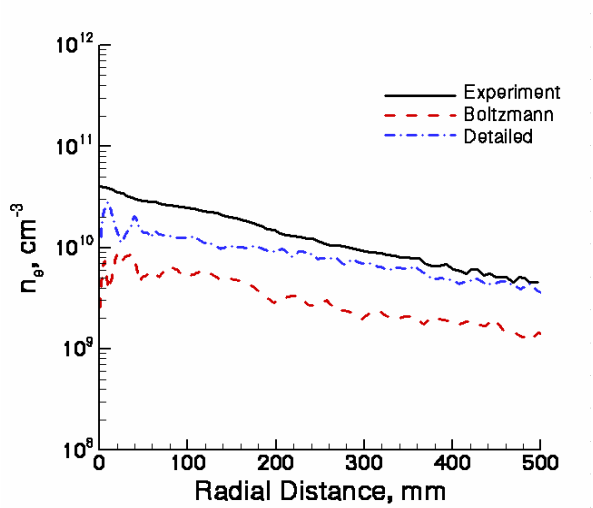

Figure 8a. Radial profiles of electron number density at 500 mm from the thruster exit plane.

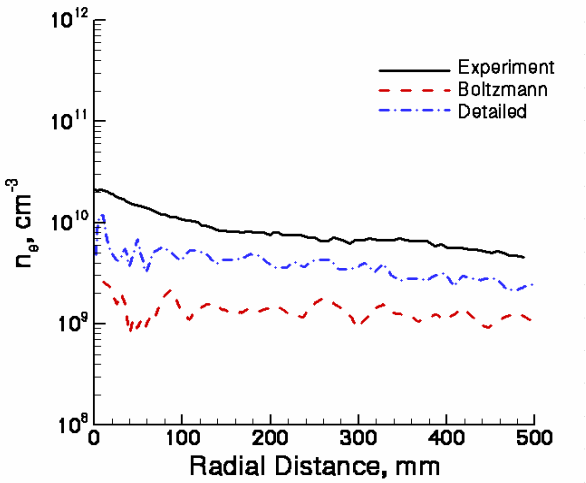

Figure 8b. Radial profiles of electron number density at 1000 mm from the thruster exit plane.

Figures 9a and 9b show radial profiles of electron temperature at distances of 10 and 50 mm from the thruster, respectively. The experimental uncertainty is reported to be ±10%.[13] Since the *Boltzmann* results are all flat lines at 10 eV, only the *Detailed model* results are provided. In general, although the *Detailed model* provides reasonable agreement with the measurements and captures the general shape, the radial gradients predicted by the model are smaller than the measured data indicate.

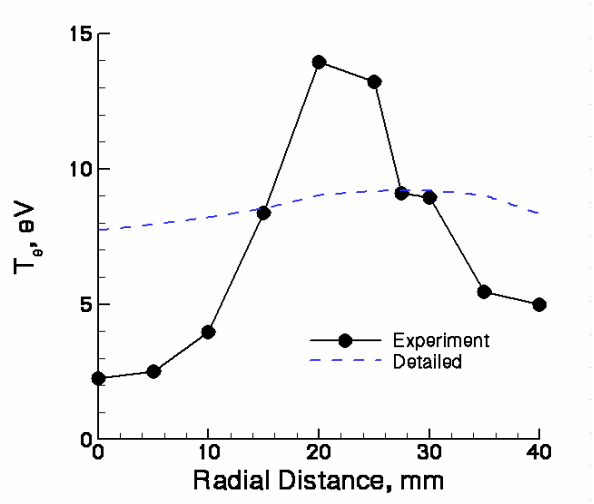

Figure 9a. Radial profiles of electron temperature at 10 mm from the thruster exit plane.

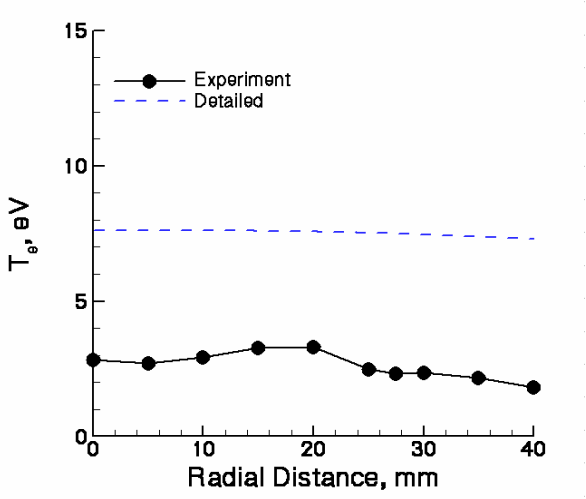

Figure 9b. Radial profiles of electron temperature at 50 mm from the thruster exit plane.

Far-field prediction of the electron temperature profiles are presented in Fig. 10. The measured data were obtained by Zakharenkov et al.[16] and the simulations use the second set of operating conditions given in Table 1. It is clearly shown that the *Detailed model* gives good agreement with the measured data in the far field.

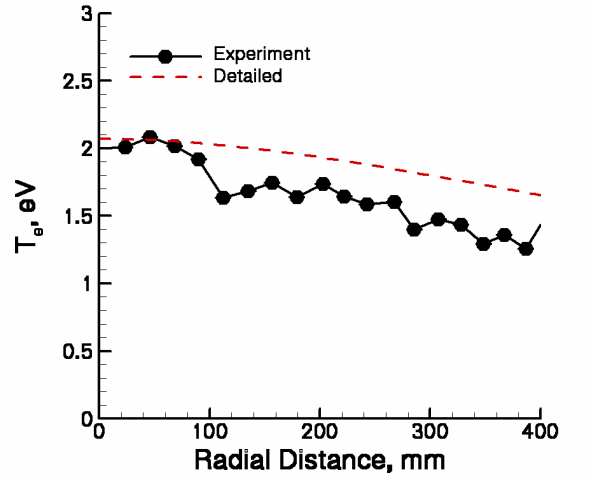

Figure 10. Radial profiles of electron temperature at an axial distance of 500 mm from the thruster.

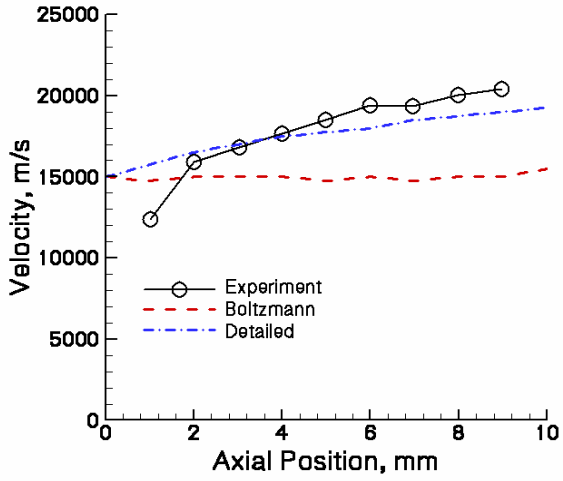

Figure 11. Axial components of velocity at a radial position of 27.5 mm.

Finally, the simulation results are compared with Laser Induced Fluorescence (LIF) measurements of Xe^+ axial velocity component obtained by Keefer et al.[17] in the near field plume. In Ref. 17, it is explained that the reported velocity data represent the central value of the ion velocity distribution functions detected by the LIF diagnostic. Therefore, for consistency with the experiment, the ion velocity distribution function is calculated throughout the flow field, and the most probable value of the distributions obtained. Figure 11 shows the axial velocity profiles at a radial position of 27.5 mm which is along the thruster channel center. The simulations use the third set of operating

conditions given in Table 1. It is clear that the *Boltzmann model* fails to produce sufficient ion acceleration in the near field of the plume. As discussed with reference to Figs. 2a and 2b, the *Detailed model* predicts strong ion acceleration in the near field region and rapidly accelerates the ions from the thruster exit velocity of 15 km/s to a value of about 20 km/s that corresponds to the measured data.

IV.Conclusions

A hybrid particle-fluid PIC-DSMC model using both a *Detailed model* and the *Boltzmann model* for the fluid electrons was applied to simulate the plume flow from a D55 anode layer Hall thruster. Generally, the *Detailed model* provided better results than the *Boltzmann model*. The *Detailed model* accurately predicted the extended ion acceleration region outside the thruster. By comparison, the *Boltzmann model* indicated almost no ion acceleration outside the thruster. The simulation results of the *Detailed model* and the *Boltzmann model* underpredicted the electron number density, especially in the far-plume field. This disparity may be caused by the simulated electric fields being too strong and leading to overacceleration of the ions. One possible mechanism that should be included in future work is partial confinement of electrons by the magnetic field of the thruster leaking into the plume. Future work will also involve modeling the D55 thruster plasma to generate improved thruster exit flow conditions.

Acknowledgments

This work is supported by NASA Grant NNC04CB15C. The authors gratefully acknowledge the contributions to this work by Dr. Chunpei Cai for discussions.

References

[1]Marrese, C. M., Frisbee, R., Sengupta, A., Cappelli, M. A., Tverdoklebov, S., Semenkin, S., and Boyd, I. D., "Very High I_{sp} Thruster with Anode Layer (VHITAL): An Overview," *AIAA Paper* 2004-5910, July 2004.

[2]Bird, G. A., *Molecular Gas Dynamics and the Direct Simulation of Gas Flows,* Oxford Press, New York, 1994.

[3]Birdsall, C. K., and Langdon, A. B., *Plasma Physics Via Computer Simulation*, Adam Hilger, New York, 1991.

[4]Keidar, M., Choi, Y., and Boyd, I. D., "Modeling a Two-Stage High-Power Bismuth Anode Layer Thruster and its Plume," *IEPC Paper* 2005-045, October 2005.

[5]Boyd, I. D., "Computation of the Plume of an Anode-Layer Hall Thruster," *Journal of Propulsion and Power*, Vol. 16, No. 5, 2000, pp. 902-909.

[6]Boyd, I. D. and Yim, J. T., "Modeling of the Near Field Plume of a Hall Thruster," *Journal of Applied Physics*, Vol. 95, 2004, pp. 4575-4584.

[7]Cai, C., and Boyd, I. D., "3D Simulation of Plume Flows from a Cluster of Plasma Thrusters," *AIAA Paper* 2005-4662, July 2005.

[8]Dietrich, S. and Boyd, I. D., "Scalar and Parallel Optimized Implementation of the Direct Simulation Monte Carlo Method", *J. of Computational Physics*, Vol. 126, 1996, pp. 328-342.

[9]Ahedo, E., Martinez-Cerezo, P., and Martinez-Sanchez, M., "One-dimensional Model of the Plasma Flow in a Hall Thruster," *Physics of Plasma*, Vol. 8, 2001, pp. 3058-3068.

[10]Mitcher, M., and Kruger, C. H., *Partially Ionized Gases*, Wiley, 1973.

[11]Pullins, S. H., Chiu, Y., Levandier, D. J., and Dresseler, R. A., "Ion Dynamics in Hall Effect and Ion Thruster – Xenon Symmetric Charge Transfer," *AIAA Paper* 2000-0636, January 2000.

[12]Miller, S., Levandier, D. J., Chiu, Y., and Dresseler, R. A., "Xenon Charge Exchange Cross Sections for Electrostatic Thruster Models," *Journal of Applied Physics*, Vol. 19, 2002, pp. 984-991.

[13]Domonkos, M. T., Marrese, C. M., Haas, J. M., and Gallimore, A. D., "Very Near-Field Plume Investigations of the D55," *AIAA Paper* 97-3062, July 1997.

[14]Gulczinski, F. S., Gallimore, A. D., Carlson, D. O., and Gilchrist, B. E., "Impact of Anode Layer Thruster Plumes on Satellite Communications," *AIAA Paper* 97-3067, July 1997.

[15]Semenkin, A., Kochergin, A., Garkusha,V., Chislov, G., Rusakov, A., Tverdoklebov, S., and Sota, C., "RHETT/EPDM Flight Anode Layer Thruster Development," *IEPC Paper* 97-106, August 1997

[16]Zakharenkov, L., Semenkin, A. V., and Lebedev, Y. V., "Measurement Features and Results of TAL D-55 Plume," *IEPC Paper* 2005-184, October 2005.

[17]Keefer, D., Wright, N., Hornkohl, J. O., and Bangasser, J., "Multiplexed LIF and Langmuir Probe Diagnostic Measurements in the TAL D-55 Thruster," *AIAA Paper* 97-2425, July 1999.

[18]Keidar, M., and Boyd, I. D., "Effect of a magnetic field on the Plasma Plume from Hall Thrusters," *Journal of Applied Physics*, Vol. 86, No. 9, 1999, pp. 4786-4791.